The Stability of Relativistic Neutron Stars in Binary Orbit

T. W. Baumgarte[1], G. B. Cook[2], M. A. Scheel[2], S. L. Shapiro[1,3] and S. A. Teukolsky[2,4]

[1] *Department of Physics, University of Illinois at Urbana-Champaign, Urbana, Il 61801*
[2] *Center for Radiophysics and Space Research, Cornell University, Ithaca, NY 14853*
[3] *Department of Astronomy and NCSA, University of Illinois at Urbana-Champaign, Urbana, Il 61801*
[4] *Departments of Physics and Astronomy, Cornell University, Ithaca, NY 14853*

We analyze the stability of relativistic, quasi-equilibrium binary neutron stars in synchronous circular orbit. We explore stability against radial collapse to black holes prior to merger, and against orbital plunge. We apply theorems based on turning points along uniformly rotating sequences of constant angular momentum and rest mass to locate the onset of secular instabilities. We find that inspiraling binary neutron stars are stable against radial collapse to black holes all the way down to the innermost stable circular orbit.

PACS numbers: 04.20.Ex, 04.25.Dm, 04.30.Db, 04.40.Dg, 97.60.Jd

The two-body problem is one of the outstanding, unsolved problems in classical general relativity. However, neutron star binary systems are known to exist, even within our own galaxy [1]. Binary systems are among the most promising sources for gravitational wave detectors now under construction, like LIGO, VIRGO and GEO. This has motivated an intense theoretical effort to predict the gravitational wave form emitted during the inspiral and coalescence of two neutron stars.

Fully general relativistic treatments of the problem are complicated by the nonlinearity of Einstein's equations and the need for very large computational resources [2]. Recently, Wilson and Mathews [3] reported preliminary results obtained with a relativistic numerical evolution code. Their dynamical calculations suggest that the neutron stars may collapse to black holes before their orbit becomes unstable and the stars plunge. Their results are in disagreement with predictions of Newtonian [4], post-Newtonian (PN) [5–7] and perturbation calculations [8], which show that tidal fields stabilize neutron stars against radial collapse.

In a recent paper, we presented quasi-equilibrium, polytropic models of fully relativistic, equal mass neutron star binaries in synchronous circular orbits [9]. In Newtonian gravity, strict equilibrium exists for two stars in circular orbit. In general relativity, because of the emission of gravitational waves, binaries cannot be in strict equilibrium. However, outside of the innermost stable circular orbit (ISCO), the timescale for orbital decay by radiation is much longer than the orbital period, so that the binary can be considered to be in "quasi-equilibrium". This fact allows us to neglect both gravitational waves and wave-induced deviations from a circular orbit to very good approximation. A detailed discussion of our approximations and numerical method will be presented in a forthcoming paper [10].

In [9], we focused on the construction of quasi-equilibrium models, but did not discuss their stability. We found that the maximum allowed mass slightly *increases* as the separation of the stars decreases. In this Letter we construct sequences of constant angular momentum and sequences of constant rest mass, which then allows us to apply rigorous theorems based on turning-points along the sequences to locate the onset of secular instabilities. We find that neutron stars in synchronous orbit are stable against radial collapse to black holes until they encounter the orbital instability at the ISCO.

Applying turning-point methods to binaries in corotation allows us to detect *secular* instabilities. The separation at which simultaneous extrema exist in the mass-energy and the angular momentum curves marks the point along an evolutionary sequence at which the binary becomes unstable in the presence of some dissipative mechanism. This instability is distinct from *dynamical* instability, which arises independently of any dissipation and grows on a dynamical timescale. Gravitational radiation can drive the secular instability [11], which is expected to occur before (i.e. at larger separation than) the onset of a dynamical instability [4,12]. It is therefore anticipated that it is the secular instabilities that limit the range of stable configurations.

Because of finite numerical resources, we cannot construct models of very large separation. We therefore observe the increase of the maximum mass only for separations smaller than about 4 stellar radii. However, even at this separation, tidal effects are still fairly small. Moreover, PN calculations, which are valid for larger separations, suggest that the maximum mass should also increase monotonically with decreasing separation [5,7]. In the following we will therefore assume that the maximum allowed mass monotonically increases as the separation decreases.

For a given equation of state, cold equal mass binary neutron stars in synchronous circular orbit form a two-parameter family, just like single, uniformly rotating stars. In our numerical code we adopt the central density and relative separation to uniquely specify a particular configuration. A Lemma by Friedman, Ipser and

Sorkin [12], originally derived for single, uniformly rotating stars, can therefore be adapted to corotating binaries:

LEMMA. *Consider a two-parameter family of equal mass binary stars in synchronous circular orbits based on an equation of state of the form $P = P(\rho_0)$. Suppose that along a continuous sequence of models labeled by a parameter λ, there is a point λ_0 at which both $\dot{M}_0 \equiv dM_0/d\lambda$ and $\dot{J}$ vanish and where $d(\dot{\Omega}\dot{J} + \dot{\mu}\dot{M}_0)/d\lambda \neq 0$. Then the part of the sequence for which $(\dot{\Omega}\dot{J} + \dot{\mu}\dot{M}_0) > 0$ is unstable for λ near λ_0.*

Here P is the pressure, ρ_0 the rest-mass density, J and M_0 are the angular momentum and rest (baryon) mass of one of the two stars, Ω the angular velocity and μ is the chemical potential. We will later use M for the total mass-energy of one of the two stars (that is half the total ADM mass of the spacetime). The proof of the Lemma follows directly from Theorem 1 of [13]. In practice it is more useful to apply the following related Theorem:

THEOREM 1. *Consider a continuous sequence of equal mass binary stars in synchronous circular orbits based on an equation of state of the form $P = P(\rho_0)$. Suppose that the total angular momentum is constant along the sequence, and that there is a point λ_0 where $\dot{M}_0 = 0$ (and where $\mu > 0$, $d(\dot{\mu}\dot{M}_0)/d\lambda \neq 0$). Then the part of the sequence for which $\dot{\mu}\dot{M}_0 > 0$ is unstable for λ near λ_0.*

The proof follows directly from the Lemma (see also [12]).

We can now apply this Theorem to our numerical models. In these models the matter obeys a polytropic equation of state, $P = K\rho_0^{1+1/n}$, where K is constant and n is the polytropic index. Note that physical dimensions enter the problem only through K. It is therefore convenient to introduce the dimensionless quantities $\bar{\rho}_0 = K^n\rho_0$, $\bar{M}_0 = K^{-n/2}M_0$, $\bar{M} = K^{-n/2}M$ and $\bar{J} = K^{-n}J$.

In Figure 1 we plot $\bar{M}_0$ as a function of the central density $\bar{\rho}_c$ for $n = 1$. The dotted lines are curves of constant relative separation $z_A = r_{in}/r_{out}$. Here r_{in} is the inner (coordinate) distance between the two stars, as measured between the two closest points along the axis, and r_{out} is the outer distance, as measured between the most distant points along the axis. For stars in contact $z_A = 0$, and for infinitely separated stars $z_A = 1$. The lowest dotted line in Figure 1 is for stars at a separation $z_A = 0.3$, and the highest curve is for stars in contact. We expect that the Oppenheimer-Volkoff curve for infinitely separated stars lies below all these lines [14], such that the equilibrium mass supported by a given central density monotonically increases with decreasing separation.

Evolutionary inspiral sequences conserve the rest mass $\bar{M}_0$ and therefore follow horizontal lines in Figure 1. This shows, for example, that the central density $\bar{\rho}_0$ decreases as the two stars approach each other.
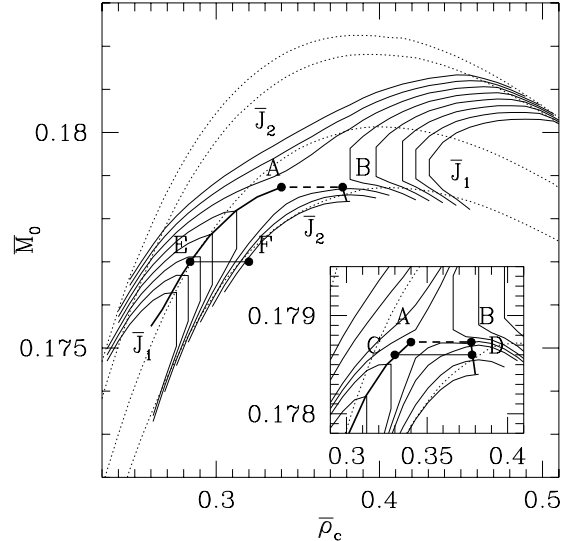
The solid lines in Figure 1 are contours of constant

FIG. 1. Contours of constant angular momentum in a rest-mass versus central density diagram. The dotted lines are sequences of constant relative separation z_A, ranging from 0.3 (bottom curve) to 0 (touching stars, top curve). The thin solid lines are contours of constant angular momentum, ranging from $\bar{J}_1 = 0.049$ to $\bar{J}_2 = 0.0498$ in increments of 0.0001. In the insert we also show contours for $\bar{J} = 0.04955$ and 0.049575. The thick solid lines mark the onset of secular instabilities (see text).

total angular momentum $\bar{J}$. The angular momentum of infinitely separated binaries is infinite, and decreases for approaching binaries. There is a critical angular momentum $\bar{J}^{crit}$, for which the contours form a saddle point (point A). This critical angular momentum and the critical mass $\bar{M}_0^{crit}$ at the saddle point take values, which, like the maximum mass of nonrotating isolated stars, depend only on the polytropic index. For $n = 1$ we find $\bar{J}^{crit} \simeq 0.05$ and $\bar{M}_0^{crit} \simeq 0.179$ [14].

The saddle point divides the turning points of the contours into two separate classes: one for contours $\bar{J} < \bar{J}^{crit}$, and one for $\bar{J} > \bar{J}^{crit}$. We will identify the former with the instability at the ISCO, and the later with a radial instability of supramassive stars at large separations.

The class for $\bar{J} < \bar{J}^{crit}$ exists for all rest masses $\bar{M}_0 < \bar{M}_0^{crit}$ and ends at the saddle point A. The physical interpretation of these turning points can be understood by following an evolutionary sequence for a coalescing binary of fixed rest mass, which starts at a large separation, e.g., at point F. It evolves along a horizontal line, and initially both the angular momentum and the central density decrease with the separation. At point E, however, the angular momentum goes through a minimum. According to the relation [16]

$$dM = \Omega dJ + \mu dM_0, \tag{1}$$

2

this minimum has to coincide with an extremum in the total mass-energy $\bar{M}$. This extremum is well understood in Newtonian gravity (e.g. [4]), PN theory (e.g. [17]), as well as general relativity [9], and marks the onset of an orbital instability at the ISCO. Note that this orbital instability is the first instability that these binaries encounter during inspiral.

For $\bar{J} > \bar{J}^{\rm crit}$ we find a second class of turning points. This class starts at point B in Figure 1 and ends at the maximum of the OV curve for isolated, nonrotating stars [14,15]. The maximum on this limiting curve marks the onset of radial instability for isolated, nonrotating stars, and defines their maximum allowed rest mass $\bar{M}_0^{\rm max}$. By continuity, this class thus marks the onset of radial instability for supramassive sequences, consisting of stars with rest-masses $\bar{M}_0^{\rm max} < \bar{M}_0 < \bar{M}_0^{\rm crit}$. Consider, for example, a binary somewhere on the line between points C and D. Following the inspiral of these stars, they will eventually incounter the ISCO at point C. If we could reverse the inspiral and follow an evolutionary sequence towards larger separations, we know that the stars eventually have to become unstable and collapse to black holes, since their masses cannot be supported when in isolation. This will happen at the turning point D.

Note that so far we have only located turning points of contours of constant angular momentum. In order to meet all the conditions of Theorem 1 and rigorously establish the onset of a secular instability, we also need to examine the chemical potential μ. The chemical potential is not normally evaluated by a code that constructs equilibrium models (although it could be). Accordingly, it is useful to apply a different version of the Theorem that does not refer to μ:

THEOREM 2. *Consider a continuous sequence of equal mass binary stars in synchronous circular orbits based on an equation of state of the form $P = P(\rho_0)$. Suppose that the rest mass M_0 is constant along the sequence, and that there is a point λ_0 where $\dot{M} = 0$ (and where $\Omega > 0$, $d(\dot{\Omega}\dot{M})/d\lambda \neq 0$). Then the part of the sequence for which $\dot{\Omega}\dot{M} > 0$ is unstable for λ near λ_0.*

The proof follows from the Lemma together with relation (1) (see also [18]). Note that according to (1) the extrema in Theorem 1 and 2 have to coincide.

In Figure 2 we plot contours of constant rest mass $\bar{M}_0$ in an $\bar{M}$ versus $\bar{\rho}_c$ diagram. In this plot the contours describe secular evolutionary sequences. The contours again have two qualitatively different classes of extrema. One class are minima of the total energy (eg. point C), and the other are maxima (point D). The former can again be associated with the onset of an orbital instability at the ISCO, while the later mark the onset of radial instability of supramassive sequences at large separations. Both extrema end at the critical contour $\bar{M}_0^{\rm crit}$, above which the contours are monotonically decreasing for increasing ρ_c. The value of $\bar{M}_0^{\rm crit}$ agrees with the
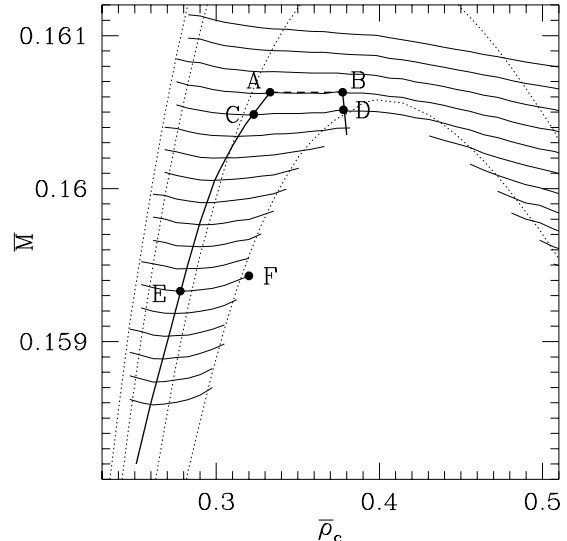

FIG. 2. Contours of constant rest mass in a mass-energy versus central density diagram. The dotted lines are sequences of constant relative separation z_A, ranging from 0.3 (bottom curve) to 0 (stars in contact, top curve). The thin solid lines are contours of constant rest mass, ranging from $\bar{M}_0 = 0.176$ to 0.1794 in increments of 0.0002. The thick solid lines mark the onset of secular instabilities (see text).

height of the saddle point A and point B in Figure 1. All extrema in Figures 1 and 2 agree to within a few percent, which is a measure of the accuracy of our numerical code.

In order to verify the assumptions in Theorem 2, we have to make sure that the extrema of the constant rest mass contours do not coincide with an extremum of the angular velocity. In Figure 3 we show the two contours connecting points E and F, and C and D, together with corresponding plots of $\bar{\Omega}$.

The minima at E and C can by analyzed very easily. Using central density as the parameter λ, all the assumptions, $\dot{M} = 0$, $\Omega > 0$ and $d(\dot{\Omega}\dot{M})/d\lambda \neq 0$ are satisfied, and we conclude that the configurations to the left of the minima, for which $\dot{\Omega}\dot{M} > 0$, are unstable. These minima mark the onset of a secular instability close to the ISCO.

The maximum at D is a little less obvious from our numerical data, since it occurs very close to a minimum in $\bar{\Omega}$. However, the offset is measureable and larger than our numerical error, and we consistently find this offset. In addition, we know that supramassive stars must become unstable when moved out from finite separation to infinite separation. We therefore conclude that the extrema in $\bar{M}$ and $\bar{\Omega}$ are indeed distinct, so that we can apply Theorem 2. This establishes the onset of a secular radial instability for the maxima on the thick line extending downward from point B in Figures 1 and 2.

We conclude that all binary configurations in the area under the thick solid lines and dashes in Figures 1 and 2
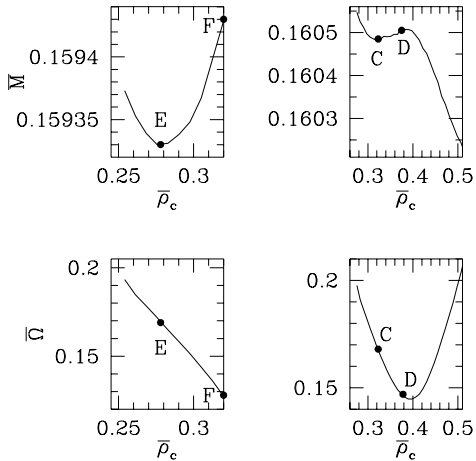
3

FIG. 3. Contours of constant rest mass. The top panels show two contours from Figure 2, and the bottom panels show the corresponding angular velocities.

are stable. This area can be subdivided into a normal and a supramassive region. All sequences with rest masses below the maximum allowed rest mass $\bar{M}_0^{\max}$ of an isolated, nonrotating star are normal sequences. These sequences start at finite separation (eg. F) and end at the ISCO (eg. E). In addition to these normal sequences, there are supramassive sequences with rest masses between $\bar{M}_0^{\max}$ and $\bar{M}_0^{\mathrm{crit}}$. Evolutionary curves for these sequences connect a radial instability at large separation (eg. D) with an orbital instability at the ISCO (eg. C). We conclude that *all normal binary neutron stars in synchronous orbit, with rest masses below the maximum for isolated, nonrotating configurations, are secularly stable against radial collapse to black holes down to the ISCO.* At the ISCO they encounter a secular orbital instability.

Supramassive stars are unstable to collapse at large separation, but, if formed at finite separation, remain stable as they inspiral down to the ISCO. Supramassive stars could arise in principle if a rapidly rotating, supramassive core were to undergo bifurcation at finite radius. Alternatively, they could arise if two spinning neutron stars become bound in a binary, or if two neutron stars accrete matter while in a binary.

The secular instability evolves on the same timescale as the inspiral, since both are driven by gravitational radiation [4,11]. Orbital plunge will occur at the onset of dynamical instability, which defines the true ISCO. Moreover, realistic binaries are more likely to be closer to irrotational (circulation = 0) than corotational [19]. For such systems, however, the location of the dynamical instability is quite close to the onset of the secular instability, both in Newtonian theory [4] and in PN theory [7]. The onset of the dynamical instability is at slightly smaller separation.

The fact that dynamical instabilities typically arise

at smaller separation than secular instabilities, together with the absence of a secular instability against radial collapse, up to the ISCO, suggests that a dynamical instability against radial collapse may also be absent in normal binary neutron stars.

[1] J. H. Taylor and J. M. Weisberg, Astrophys. J. **345**, 434 (1989); S. E. Thorsett, Z. Arzoumanian, M. M. McKinnon and J. H. Taylor, Astrophys. J. **405**, L29 (1993)

[2] K. Oohara, and T. Nakamura, Lecture delivered at Les Houches School "Astrophysical Sources of Gravitational Radiation" (Les Houches, France, Sept. 26 - Oct. 6, 1995). To be published in the Proceedings (eds. J.-A. Marck and J.-P. Lasota) (see also astro-ph/9606179)

[3] J. R. Wilson and G. J. Mathews, Phys. Rev. Lett. **75**, 4161 (1995); J. R. Wilson, G. J. Mathews and P. Marronetti, Phys. Rev. D **54**, 1317 (1996)

[4] D. Lai, F. A. Rasio, and S. L. Shapiro, Astrophys. J. Suppl. **88**, 205 (1993)

[5] D. Lai, Phys. Rev. Lett. **76**, 4878 (1996)

[6] A. D. Wiseman, submitted (gr-qc/9704018)

[7] J. C. Lombardi, F. A. Rasio and S. L. Shapiro, submitted

[8] P. R. Brady and S. A. Hughes, submitted (gr-qc/9704019)

[9] T. W. Baumgarte, G. B. Cook, M. A. Scheel, S. L. Shapiro and S. A. Teukolsky, submitted (gr-qc/9704024)

[10] T. W. Baumgarte, G. B. Cook, M. A. Scheel, S. L. Shapiro and S. A. Teukolsky, in preparation

[11] S. Chandrasekhar, Astrophys. J. **161**, 561 (1970)

[12] J. L. Friedman, J. R. Ipser and R. D. Sorkin, Astrophys. J. **325**, 722 (1988)

[13] R. D. Sorkin, Astrophys. J. **257**, 847 (1982)

[14] Computing the Oppenheimer-Volkoff curve with a very high radial resolution yields a maximum mass which is slightly *larger* than the masses of some of our binary models (see Figure 2 in [9]). However, we know from convergence tests that we *underestimate* the masses of the binary configurations by a few percent as a result of our coarse numerical grid.

[15] It is difficult to precisely locate the extrema near the saddle point with our numerical data. It may very well be that A and B actually coincide. However, this would not affect any of our conclusions about stability.

[16] J. B. Hartle, Astrophys. J. **161**, 111 (1970); J. M. Bardeen, in *Black Holes*, ed. C. DeWitt (New York: Gordon & Breach, 1972)

[17] M. Shibata, Prog. Theor. Phys. **96**, 317 (1996)

[18] G. B. Cook, S. L. Shapiro and S. A. Teukolsky, Astrophys. J. **398**, 203 (1992)

[19] L. Bildsten and C. Cutler, Astrophys. J. **400**, 175 (1992); C. S. Kochanek, Astrophys. J. **398**, 234 (1992)